NPL REPORT CIRM 13

A Calculation of the water to graphite perturbation factor ratios for the NACP type 02 ionisation chamber using Monte Carlo techniques.

A J Williams M R McEwen
and A R DuSautoy
Centre for Ionising Radiation Metrology

June 1998

CIRM 13

JUNE 1998

A calculation of the water to graphite perturbation factor ratios for the NACP type 02 ionisation chamber using Monte Carlo techniques.

A J Williams M R McEwen and A R DuSautoy
Centre for Ionising Radiation Metrology
National Physical Laboratory
Teddington
Middlesex
United Kingdom TW11 0LW

ABSTRACT

Calculations have been made of the water to graphite perturbation factor ratio for the NACP type 02 ionisation chamber at energies of 4, 8, 12, and 19 MeV. Within the uncertainties of the calculation, the ratio of the perturbation due to the cavity effect was found to be unity at all energies, whilst the ratio of the perturbation due to the wall effect was found to be unity at 19 MeV, decreasing to 0.99 at 4 MeV. It is likely that the wall effect results have a significant systematic uncertainty due to the poor back-scatter modelling of the EGS code used to perform the calculations.

ISSN 1369-6793

National Physical Laboratory
Teddington, Middlesex, UK, TW11 0LW

Approved on behalf of Managing Director, NPL,
by J Hunt, Head of Centre, Centre for Ionising Radiation Metrology

CONTENTS

FIGURES

TABLES

1. INTRODUCTION

Over several years NPL has been developing a calibration service for electron beam radiotherapy. This is based on the primary standard electron-beam graphite calorimeter and yields a direct calibration of an ionisation chamber in terms of absorbed dose to water[1]. The theoretical basis of the calibration service requires that the ratio of perturbation factors be known for the reference ionisation chambers used in the service, namely the NACP type 02 ionisation chamber (a plane parallel chamber with a 10 mm diameter, 2 mm deep sensitive air volume: see **Figure 1**). It has generally been assumed that the NACP chamber has a perturbation factor of unity. However, as described previously by Nahum[2], evidence is increasingly coming to light which indicates that this may not be the case at all energies. For example, Ma and Rogers[3] recently performed Monte Carlo calculations to simulate the effect of the wall materials in the NACP chamber on the chamber response. They obtained a value for the wall perturbation factor, p_{wall}, at the depth of maximum ionisation, d_{max}, in a water phantom for a 4 MeV beam of 1.014 ± 0.004. As a result of this increasing uncertainty in the value of the perturbation factor for the NACP chamber, it was decided to calculate this ratio directly using Monte Carlo techniques. This would help ensure that the overall uncertainty of the new calibration service was minimised.

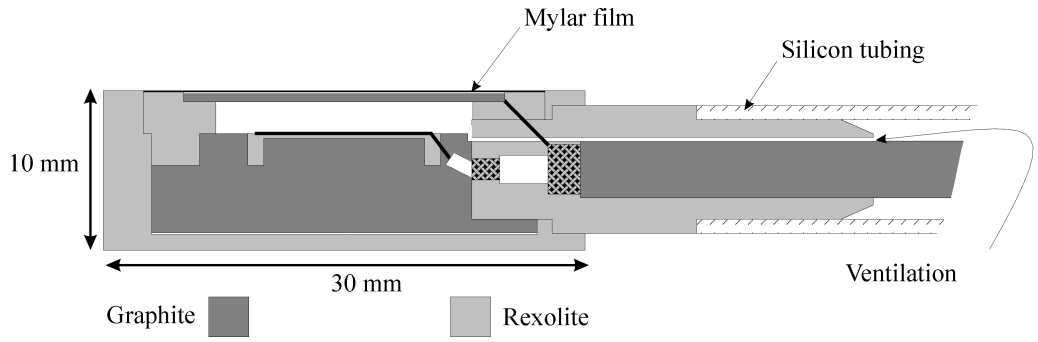

Figure 1 NACP Type 02 Ionization Chamber

2. DEFINITION OF THE PERTURBATION FACTOR

In the discussion which follows, beam quality q (defined by the half value depth in water) can be related to a reference measurement depth d_m in a medium m which is irradiated by an electron beam. The reference measurement depth d_w for water is defined by

$$d_w = 0.5 \times R_{50,w} - 0.1 \qquad (1)$$

and d_w for graphite by

$$d_g = d_w \times \frac{R_{50,g}}{R_{50,w}} \qquad (2)$$

where $R_{50,w}$ and $R_{50,g}$ are the half value depths for water and graphite.

In the Spencer-Attix formulation of cavity ionization theory[4], the absorbed dose $D_{m,q}$ to the medium m at beam quality q is related to the mean absorbed dose $D_{air,q}$ to an air cavity positioned with its effective point of measurement at the same point, according to

$$\frac{D_{m,q}}{D_{air,q}} = \frac{\int_{\Delta}^{E_{\max}} \Phi_{m,q}(E)\, L_m^{\Delta}(E)\, dE + TE}{\int_{\Delta}^{E_{\max}} \Phi_{air,q}(E)\, L_{air}^{\Delta}(E)\, dE + TE} \tag{3}$$

where $\Phi_{m,q}(E)$ is the electron fluence spectrum at the reference point in the absence of the ion chamber, and $\Phi_{air,q}(E)$ is the electron fluence spectrum in the air cavity. The mono-energetic restricted stopping powers $L_m^{\Delta}(E)$ and $L_{air}^{\Delta}(E)$ at energy E are evaluated with a cut-off energy Δ. The terms TE (Track-End terms) account for interactions in which electrons drop below Δ and are equal to

$$TE = \Phi_{m,q}(\Delta)\, L_m^{\Delta}(\Delta)\, \Delta$$

E_{max} is an end-point energy which may be taken to be the maximum accelerator energy.

The undisturbed electron fluence $\Phi_{m,q}(E)$ can be calculated using Monte Carlo simulation techniques, which allows the evaluation of the numerator in equation **(3)**. However, in general, the disturbed fluence $\Phi_{air,q}(E)$ in the air cavity of an arbitrary ion chamber is not known. This can be accounted for by expressing equation **(3)** as

$$\frac{D_{m,q}}{D_{air,q}} = \frac{\int_{\Delta}^{E_{\max}} \Phi_{m,q}(E)\, L_m^{\Delta}(E)\, dE + TE}{\int_{\Delta}^{E_{\max}} \Phi_{m,q}(E)\, L_{air}^{\Delta}(E)\, dE + TE} \cdot \frac{\int_{\Delta}^{E_{\max}} \Phi_{m,q}(E)\, L_{air}^{\Delta}(E)\, dE + TE}{\int_{\Delta}^{E_{\max}} \Phi_{air,q}(E)\, L_{air}^{\Delta}(E)\, dE + TE} \tag{5}$$

which can be written as

$$\frac{D_{m,q}}{D_{air,q}} = \bar{s}_{m/air,q}\, p_q \tag{6}$$

where the ratio of mean stopping powers $\bar{s}_{m/air,q}$ is defined by

$$\bar{s}_{m/air,q} = \frac{\int_{\Delta}^{E_{\max}} \Phi_{m,q}(E)\, L_m^{\Delta}(E)\, dE + TE}{\int_{\Delta}^{E_{\max}} \Phi_{m,q}(E)\, L_{air}^{\Delta}(E)\, dE + TE} \tag{7}$$

and the corresponding perturbation factor p_q is defined by

$$p_q = \frac{\int_{\Delta}^{E_{\max}} \Phi_{m,q}(E)\, L_{air}^{\Delta}(E)\, dE \; + \; TE}{\int_{\Delta}^{E_{\max}} \Phi_{air,q}(E)\, L_{air}^{\Delta}(E)\, dE \; + \; TE} \tag{8}$$

This is a strict definition of the perturbation factor p_q which is consistent with the evaluation of the stopping power ratio according to equation **(5)**. In other words, the use of the undisturbed fluence in the evaluation of the medium over air stopping power ratio leads to a correction factor defined by equation **(8)**.

To date there have been no full Monte Carlo calculations of the perturbation factor as defined by equation **(8)**. The more familiar approach is to split the perturbation factor into component parts;

$$p_q \approx p_{cav,q}\, p_{wall,q} \tag{9}$$

where, $p_{cav,q}$ accounts for the fluence disturbance due to the non-medium equivalence of the chamber air cavity, and $p_{wall,q}$ accounts for the non-medium equivalence of the chamber walls (for cylindrical chambers, a third component $p_{cel,q}$ accounts for the effect of the central electrode).

3. EVALUATION OF THE PERTURBATION FACTOR

The method of calculation outlined below allows the perturbation factor, as defined by equation **(8)**, to be evaluated directly, as well evaluating the two components $p_{cav,q}$ and $p_{wall,q}$ of the perturbation factor as defined by equation **(9)**.

In order to calculate the perturbation factor, the integrals

$$\int_{\Delta}^{E_{\max}} \Phi_{m,q}(E)\, L_{air}^{\Delta}(E)\, dE \; + \; TE \tag{10}$$

and

$$\int_{\Delta}^{E_{\max}} \Phi_{air,q}(E)\, L_{air}^{\Delta}(E)\, dE \; + \; TE \tag{11}$$

need to be evaluated. The latter integral given by equation **(11)** is simply the dose deposited in the medium, and is relatively straight forward to calculate. The Monte Carlo code EGS4[5] with user code DOSRZ could be used to evaluate this integral directly, as the NACP type 02 chamber

has RZ geometry (if we ignore the chamber stem). However, integral **(10)** is more difficult to evaluate. It requires either a specially written user code, or the user code DOSRZ to be modified, the latter being the option chosen in this case.

3.1 THE MECHANICS OF ENERGY DEPOSITION SCORING IN DOSRZ

The method of scoring energy deposited in a medium during transport of electrons and positrons in DOSRZ is relatively straight forward:

- The electron step length in the medium, *TVSTEP*, is calculated.
- The stopping power, *DEDX*, is evaluated at the initial energy of the electron in the medium.
- The energy deposited in the medium, *EDEP*, is initially calculated using the equation

$$EDEP = DEDX \times TVSTEP \tag{12}$$

- The energy deposited is later re-evaluated by taking the mean of the values of *DEDX* at the start and end of the electron step.

In order to evaluate integral **(10)**, *DEDX* has to be evaluated at the same initial electron energy as before, but in air instead of the original medium.

Energy is also deposited in the medium whenever a particle is discarded. However, with the exception of photon fluorescence, the energy deposition is the same in both media.

The actual modifications that were made to DOSRZ and associated files can be found in Appendix A.

3.2 POSSIBLE METHODS OF CALCULATION

Three possible methods of calculating the perturbation factors were identified:

Method 1 Simulate the electron histories from the point of leaving the electron linear accelerator (LINAC) exit window until the electron is discarded by EGS4.

Method 2 Split the simulation into two stages. (1) Simulate the electron histories until they almost reach the front surface of the phantom, and then save all the particle's information (position, direction, energy and weight - later referred to as phase space data) to disk. (2) continue the calculation at a later date, with the phase space data from disk being sampled more than once.

Method 3 Split the simulation into three stages. (1) and (2) as 2 above, (3) save the phase space data as it crosses a boundary near to the surface of the chamber. The calculation can then be continued using the phase space data from disk.

Method 3 provides a number of advantages over methods 1 and 2:

i. The particle spectrum saved at the front face of the phantom can be used for all the calculations, in both graphite and water, at a particular energy, thus reducing the simulation time for this part of the calculation by a factor of six.

ii. The particle spectrum saved near the boundary of the chamber can be used for all calculations in that medium at a particular energy, thus reducing the simulation times for this stage by a further factor of three.

3.3 CHOSEN METHOD OF CALCULATION

Method 3 (above) was used. For this method, two EGS4 user codes were required to calculate the perturbation factors, both of which used PRESTA[6]. The first was the NPL code ELINAC, which was used to simulate the NPL LINAC in detail (see Stage 1 below). The second was the modified version of DOSRZ (see stages 2 and 3).

3.3.1 Stage 1

ELINAC was used to create a phase space data file approximately 10 cm in front of the phantom for each of beam qualities. The electron transport parameters were set as follows: *ESTEPE* (the maximum fraction of the particle's energy that can be lost in a single step) to 0.04, *ECUT* (the energy at which an electron is discarded) to 0.611 keV, with the PEGS4 media data being created with *AE* (the lowest energy of secondary electron that can be created) set to 0.521 keV.

3.3.2 Stage 2

The stage 1 phase space data files were continued using the modified DOSRZ. As the particle data was saved to disk before it enters the chamber volume (actually as they reached the surface of the NACP chamber), the DOSRZ input file was relatively simple, as the intricate geometry of the NACP chamber did not need to be coded (see **Figure 2**). Two calculations were made for

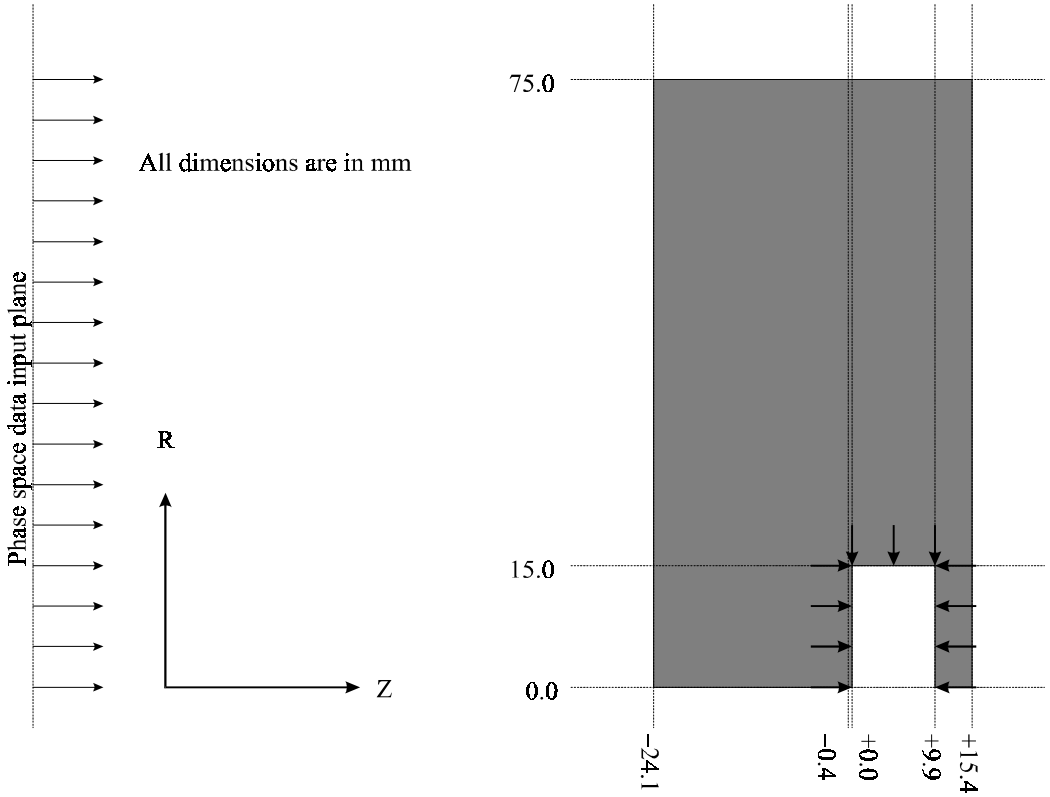

Figure 2 Stage 2 geometry setup, shown for 19 MeV electrons in graphite

each energy, one in a water phantom, one in a graphite phantom, with the stage 1 phase space data over-sampled fifty times for each calculation. *ESTEPE* was set to the default 0.00 (ie., 100%).

Ideally, *ECUT* would have been set on a region by region basis, however, DOSRZ V10 (the latest PC version) did not allow this. As electron transport down to 0.521 keV is important in this stage of the calculation for parts of the geometry, *ECUT* was set to this value. However, this does greatly increase the time of the simulation, so in order to increase its efficiency, zonal rejection was used: PEGS4 data was created with an *AE* of 0.521 keV for region 3 (directly in front of the scoring region where more accurate electron transport was required), and 0.711 keV for all the other regions. This has a similar effect to using variable *ECUT*s.

3.3.3 Stage 3

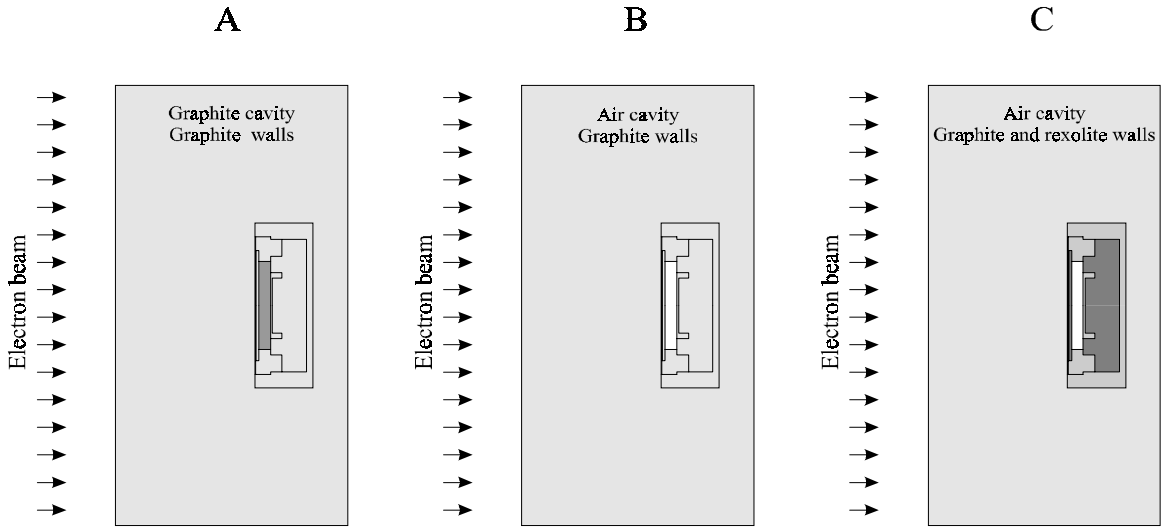

Figure 3 Three geometry set-ups for stage 3

In order to calculate $p_{cav,q}$ $p_{wall,q}$ and p_q as defined by equations **(8)** and **(9)**, three calculations were required in each medium for each beam quality, as shown in **Figure 3**, where, geometry A is for the evaluation of equation **(10)** in a homogeneous phantom (the wall geometries of the NACP chamber were coded into the calculation, but the wall media were set to graphite or water), geometry B is for the evaluation of equation **(11)** in a homogenous phantom, and geometry C is for the evaluation of equation **(11)**, but in a non-homogenous phantom (the wall geometries and media of the NACP chamber were coded into the calculation). $p_{cav,q}$, $p_{wall,q}$ and p_q can then be calculated by taking the ratios:

$$p_{cav,q} = \frac{A}{B} \tag{13}$$

$$p_{wall,q} = \frac{B}{C} \tag{14}$$

$$p_q = p_{cav,q} \times p_{wall,q} = \frac{A}{B} \times \frac{B}{C} = \frac{A}{C} \tag{15}$$

The stage 2 phase space data files were continued, again using the modified version of DOSRZ. Geometry coding for this stage was more intricate than for the previous one (see **Figure 4**). The stage 2 phase space data was typically over-sampled eight times.

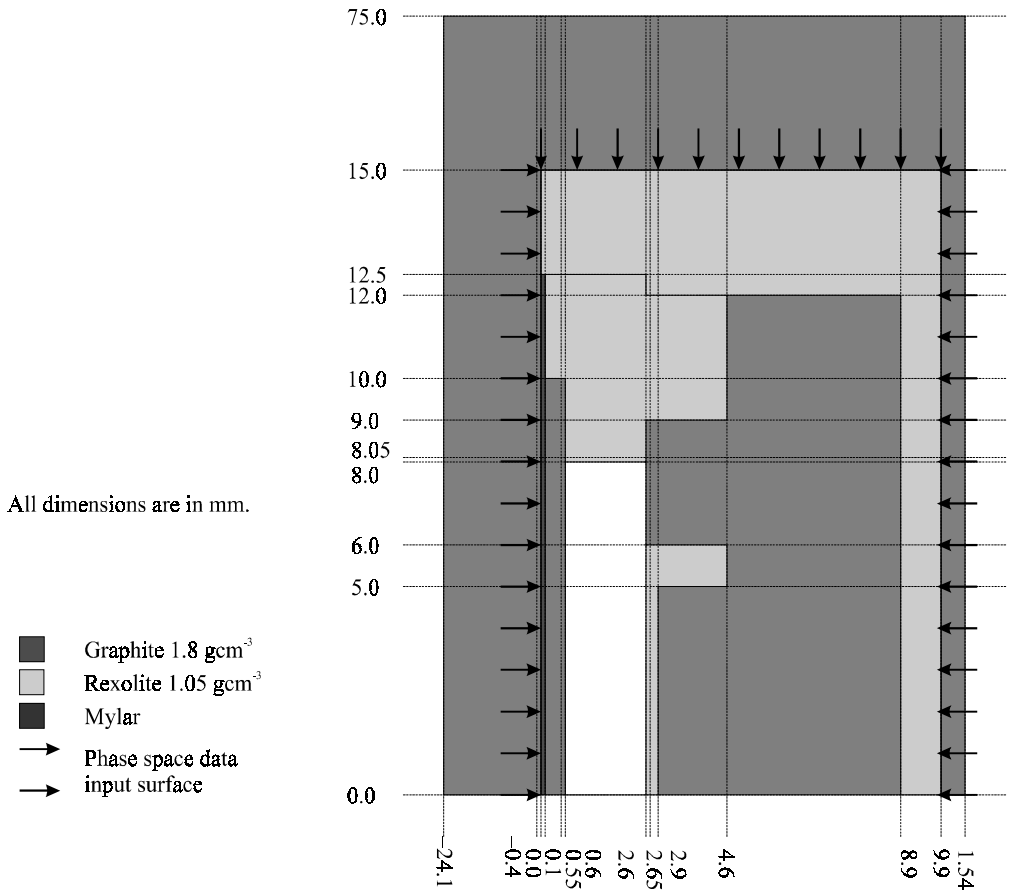

Figure 4 Stage 3 geometry setup, shown for 19 MeV electrons in graphite

As for stage 2, ideally, *ECUT* would have been set on a region by region basis. As electron transport down to 0.512 keV is important in parts of the geometry for this stage of the calculation, *ECUT* was set to this value. As before, zonal rejection was used: PEGS4 data was created with an *AE*'s of 0.512 keV, 0.521 keV, and 0.711 keV.

3.4 METHOD OF ANALYSIS

DOSRZ uses, by default, ten 'bins' in which to score dose data, the dose in each bin being independent from that in all other bins. Statistical analysis is performed on these bins resulting in mean dose scored, and the standard error on the mean.

A simple way of evaluating equation **(8)** would be to take the ratio of the mean dose scored from the two calculations, and to calculate the standard error by taking the quadrature error. However, advantage can be taken of the correlation between the two simulations by taking the ratio of doses in each bin and then calculating the standard error as in equations **(16)** and **(17)**,

$$variance = \frac{1}{n}\sum_{i=0}^{i=n}\left|\frac{dose[1]_i}{dose[2]_i} - mean\left(\frac{dose[1]_i}{dose[2]_i}\right)\right|^2 \quad (16)$$

$$\sigma_{st\ err} = \sqrt{\frac{variance}{n-1}} \quad (17)$$

where, n is the number of statistical bins, $dose[1]_i$ is the dose scored in the i^{th} bin for the 1st calculation, and $dose[2]_i$ is the dose scored in the i^{th} bin for the 2nd calculation. Calculating the standard error using this method results in an improved estimate of the standard error over taking the quadrature sum of the errors by between a factor of three and six. In theory, this translates to a reduction in the simulation times by a factor of between 9 and 36. In practice, the efficiency gain is greater than this: the uncertainties calculated using the quadrature sum being limited by the finite size (or inherent noise) of the input phase space data file.

3.5 RESULTS

3.5.1 Cavity Effect

The results of the calculation of the cavity effect are shown in **Table 1** and **Figure 5** below (the plotted data points have been spread out around the nominal energies to allow for easier viewing).

Nominal Energy (MeV)	$p_{cav,\ water}$	Uncertainty (1σ%)	$p_{cav,\ graphite}$	Uncertainty (1σ%)	$\frac{p_{cav,\ water}}{p_{cav,\ graphite}}$	Uncertainty (1σ%)
4	1.0003	0.16	0.9969	0.28	1.0033	0.32
8	0.9975	0.15	0.9955	0.26	1.0021	0.30
12	0.9983	0.34	0.9963	0.32	1.0020	0.47
19	1.0006	0.26	0.9949	0.43	1.0058	0.50

Table 1 Cavity effect results

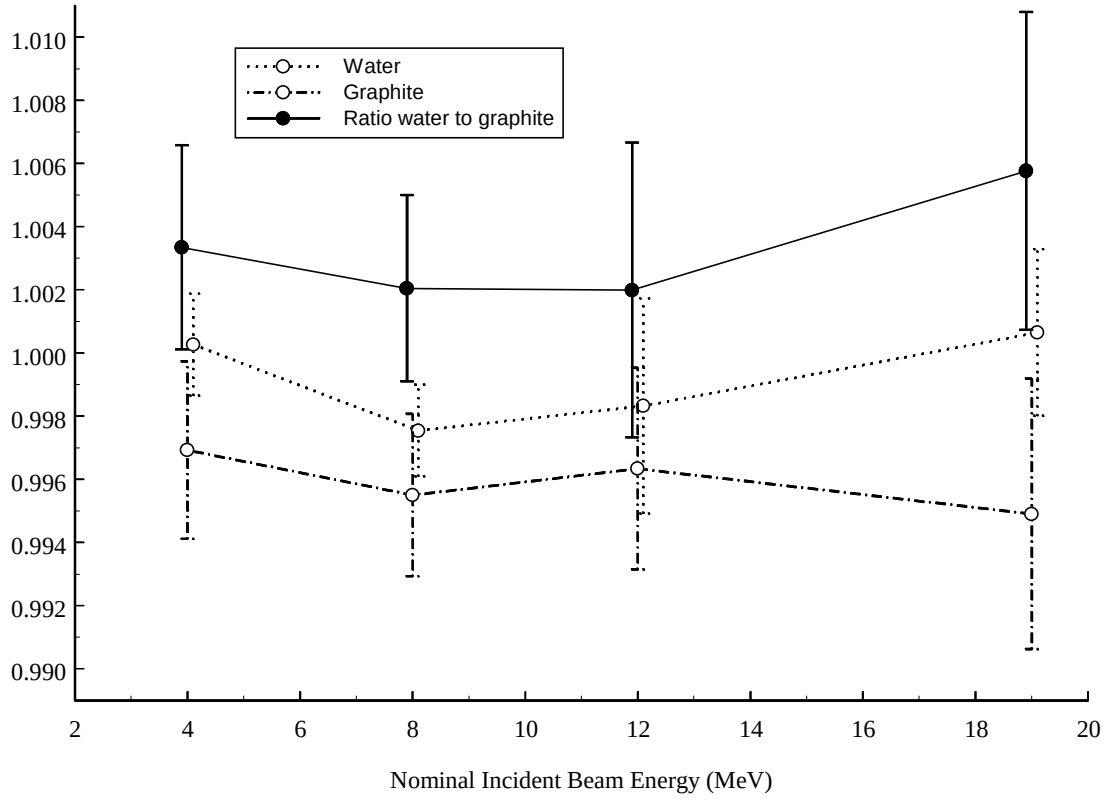

Figure 5 Cavity Effect Results

3.5.2 Wall Effect

The results of the calculation of the wall effect are shown in **Table 2** and **Figure 6** below.

Nominal Energy (MeV)	$p_{wall,\ water}$	Uncertainty (1σ%)	$p_{wall,\ graphite}$	Uncertainty (1σ%)	$\frac{p_{wall,\ water}}{p_{wall,\ graphite}}$	Uncertainty (1σ%)
4	1.0127	0.21	1.0268	0.27	0.9863	0.35
8	1.0114	0.32	1.0178	0.16	0.9937	0.35
2	1.0079	0.31	1.0136	0.41	0.9944	0.51
19	1.0065	0.47	1.0124	0.47	0.9942	0.67

Table 2 Wall effect results

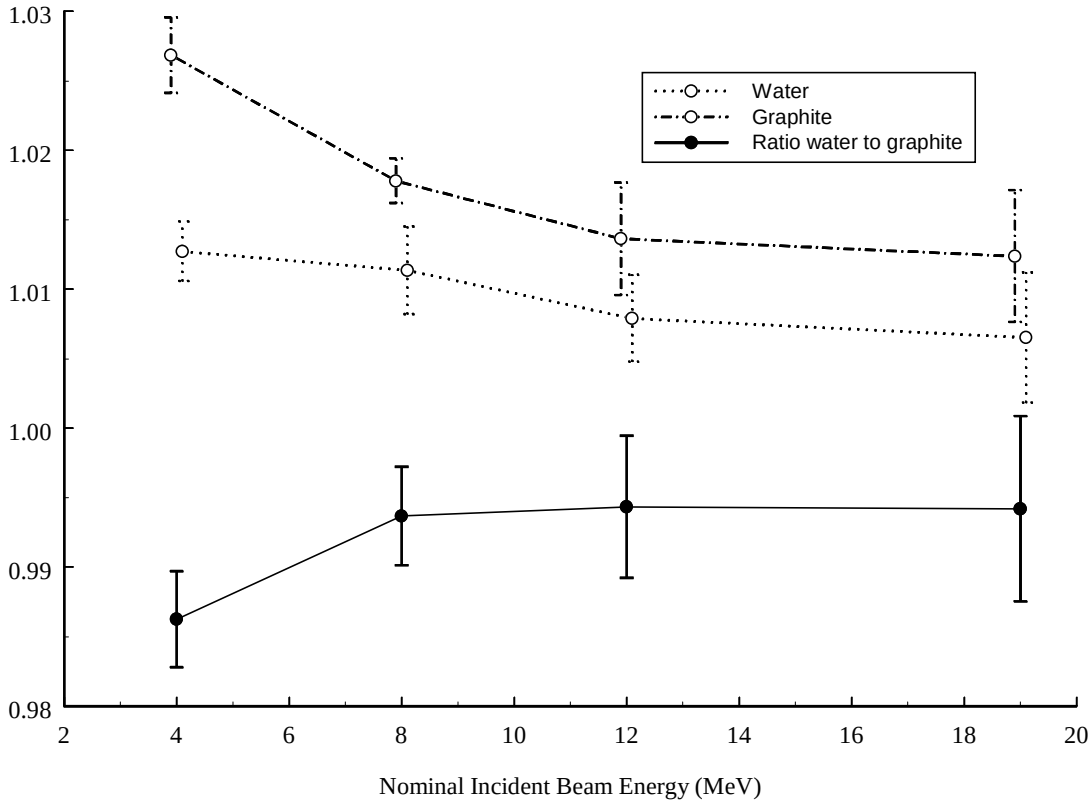

Figure 6 Wall Effect Results

3.5.3 Total Perturbation

The total perturbation factor p_q is not calculated by multiplying $p_{cav,q}$ by $p_{wall,q}$ but it is evaluated directly using equation **(15)**. This has the effect of reducing the estimate of the uncertainty in the calculation by a factor of 1.3 and 2, depending on energy. The results of the calculation of the total perturbation are shown in **Table 3** and in **Figure 7**.

Nominal Energy (MeV)	p_{water}	Uncertainty (1σ%)	$p_{graphite}$	Uncertainty (1σ%)	$\frac{p_{water}}{p_{graphite}}$	Uncertainty (1σ%)
4	1.0130	0.12	1.0237	0.20	0.9896	0.24
8	1.0089	0.30	1.0132	0.18	0.9957	0.36
12	1.0062	0.32	1.0099	0.23	0.9963	0.39
19	1.0072	0.38	1.0072	0.31	0.9999	0.50

Table 3 Total perturbation

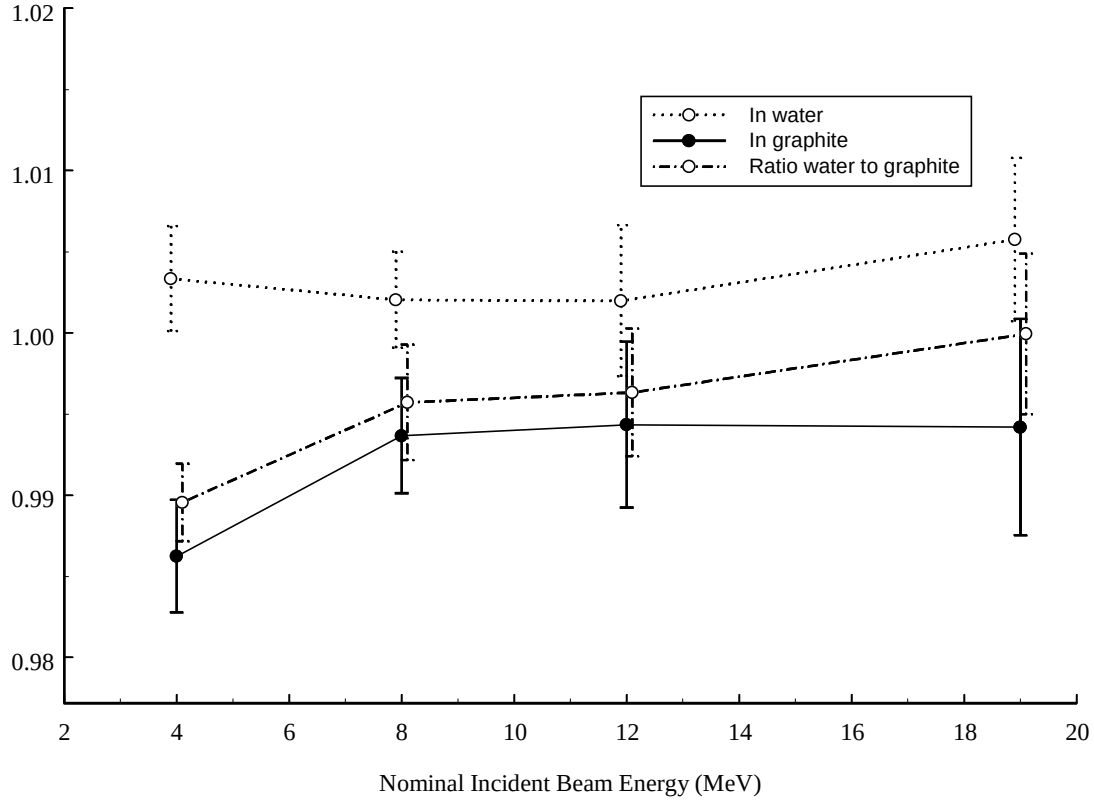

Figure 7 Total Perturbation Results

3.6 DISCUSSION ON RESULTS OF CALCULATIONS

3.6.1 Cavity Effect

For a well guarded chamber, such as the NACP, it has generally been assumed that $p_{cav,\,q}$ is unity, for energies down to ≈ 2 MeV at depths close to d_{max}. The results of these calculations appear to confirm this assumption, with p_{cav} being very close to unity at all energies.

Note: For the purposes of this calculation, it has been assumed that, as the only difference between the two simulations required in each medium to calculate the ratio $p_{cav,\,medium}$ is the change in stopping power of the medium in the cavity, any systematic errors present in the EGS4 code will to a large extent cancel.

3.6.2 Wall Effect

Introducing the NACP type 02, a predominately graphite chamber, into a water phantom, one would expect the electron fluence to be perturbed. These calculations show an increase in the dose in the cavity by a factor of 1.006 ± 0.005 at 19 MeV, increasing to 1.013 ± 0.002 at 4 MeV. As mentioned previously, Ma and Rogers[3] have calculated the wall effect for the NACP chamber at d_{max} in a 4 MeV beam with a result of 1.014 ± 0.004, in excellent agreement with these calculations.

Introducing the chamber into a graphite phantom, one would expect there to be very little change in the electron fluence. However, these calculations show a larger increase in the dose in the cavity than for the previous case in water, from 1.012 ± 0.005 at 19 MeV to 1.027 ± 0.003 at 4 MeV.

In the case of the cavity effect, it was assumed that systematic errors in EGS4, to a large degree, would cancel when ratios were taken. This assumption holds less well for the calculations of the wall effect as the change in media around the cavity will effect the amount of scatter and backscatter entering the chamber cavity, back-scatter in particular being poorly modelled by EGS. It is therefore likely that these results have a significant systematic uncertainty.

4. BACKSCATTER EXPERIMENTS.

In order to test the backscatter capabilities of EGS4, an experiment was devised in which the backscatter from various materials could be measured and compared against backscatter calculated using EGS4 code DOSRZ. This would involve measuring the ionisation current in a specially designed ion chamber with different thicknesses of materials behind the chamber, and then comparing these measurements with EGS4 calculations of the same setup.

4.1 PRELIMINARY INVESTIGATIONS

Initially, measurements were made using a Markus ionisation chamber to see if there was a measurable change in response. The Markus chamber has a very thin front wall, so in this set-up, the chamber was reversed so that the contribution to the measured ionization from the now‘rear’ wall of the chamber is minimal.

Measurements were made at the nominal energies of 12 and 19 MeV, with various thicknesses of graphite back scatter material, at 12 and 19 MeV with single thicknesses of graphite, perspex, polystyrene, and TE-plastic, and at 4 MeV with a single thickness of graphite.

4.2 RESULTS

4.2.1 Relative back-scatter measurements

Relative measurements were made at 12 and 19 MeV. The results are shown in **Table 4**. The uncertainty in the measurements was typically less than 0.1 % (1 σ).

Material	Change with respect to Polystyrene	
	19 MeV	12 MeV
Perspex	1.043	1.055
Graphite	1.059	1.067
TE-plastic	1.044	1.073

Table 4 Backscatter measurements for various materials at 12 and 19 MeV

4.2.2 Back-scatter build-up measurements

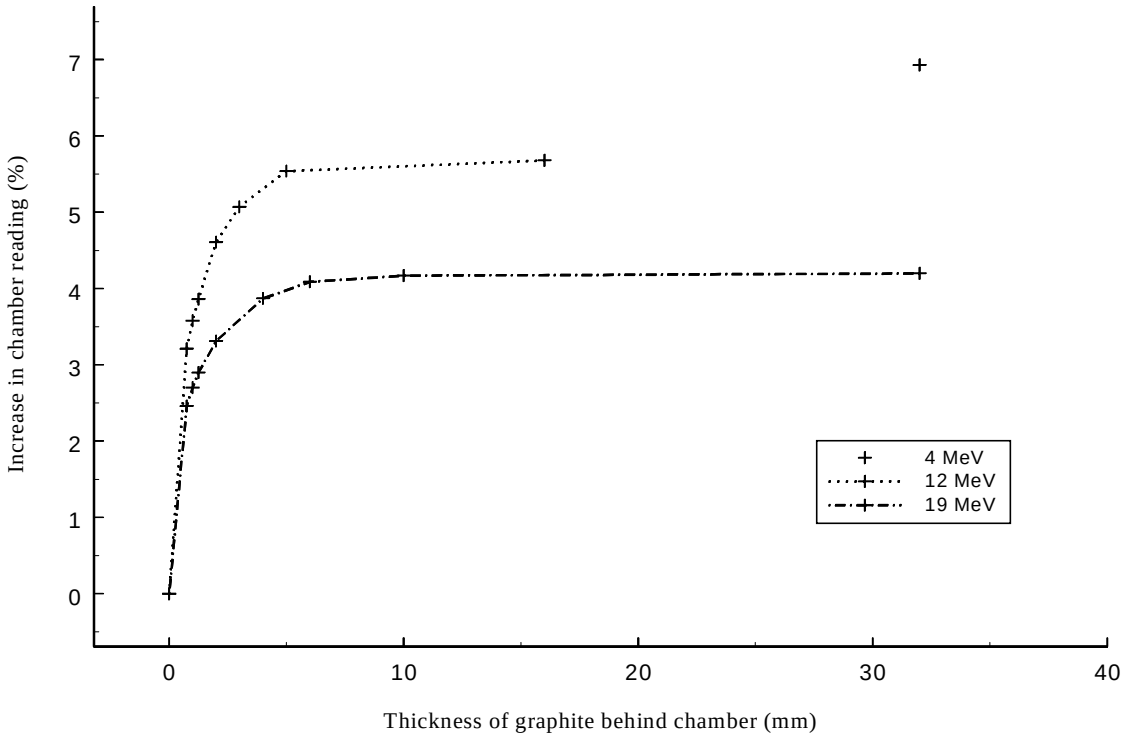

Figure 8 Backscatter buildup

The results of the back-scatter buildup measurements can be seen in **Figure 8**.Two points are quite clear from the figure: (1) backscatter increases with decreasing energy, and (2) the first 6.5 mm of graphite produces over 97% of the backscatter (6.5 mm is the thickness of graphite behind the cavity in the NACP chamber).

The above measurements clearly demonstrate that the effect of backscatter on the chamber reading can be measured. Therefore a chamber was specially designed for use in electron

energies from 4 to 19 MeV, the geometry of which could be easily simulated using Monte Carlo techniques. These simulations could then be compared against experimental backscatter measurements.

4.3 MEASUREMENTS WITH PURPOSE-BUILT CHAMBER

4.3.1 Chamber Design

The design of the chamber and phantom is shown in **Figure 9** and **Figure 10**.

The collecting electrode is made of aluminised Kapton, while the HT electrode is made of aluminised Mylar, each being stretched across an 80 mm diameter circular polystyrene frame. The chamber 'phantom' has a coin shaped cut-out for the chamber electrodes, 80 mm in diameter and 5.5 mm deep, into which the chamber electrodes, separated by a spacing ring, are placed. The chamber electrodes are held in the phantom cut out by a rear plate of 2 mm perspex, with a 60 mm diameter hole over the chamber region. The collecting volume of the chamber is 5.9 cm^3 (the cavity depth is 3 mm, the collecting electrode diameter 5 cm).

4.3.2 Experimental Results

The following experiments were carried out with full backscatter, ie., with a thickness of material behind the chamber sufficient to produce the maximum change in chamber reading. As with the experiments made with the Markus chamber, the chamber reading increases with decreasing incident beam energy (see **Table 5**), with polystyrene producing the lowest increase in chamber reading, followed by graphite, aluminium and lead. The typical uncertainty in the measurements was less than 0.1 %.

	% increase in chamber reading with respect to air			
Material	19 MeV	12 MeV	8 MeV	4 MeV
Polystyrene	1.059	1.074	1.089	1.113
Graphite	1.066	1.083	1.100	1.128
Aluminium	1.127	1.161	1.189	1.236
Lead	1.514	1.585	1.628	1.675

Table 5 Backscatter experimental measurements

Taking the ratio of the increase in measured chamber response with respect to polystyrene (**Figure 11**), graphite shows an increase in response over polystyrene of about 0.7% at 19 MeV, rising to 1.4% at 4 MeV. This is broadly consistent with the experimental measurements made by Hunt *et al*[7]

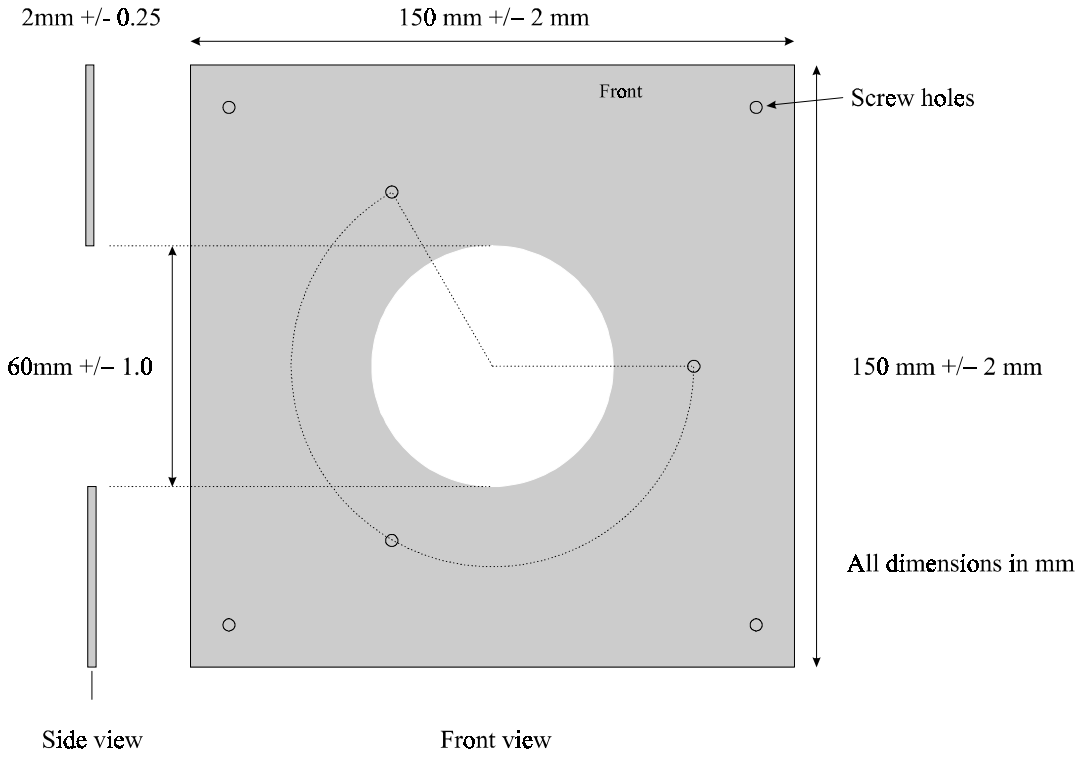

Figure 9 Backscatter chamber - top cover

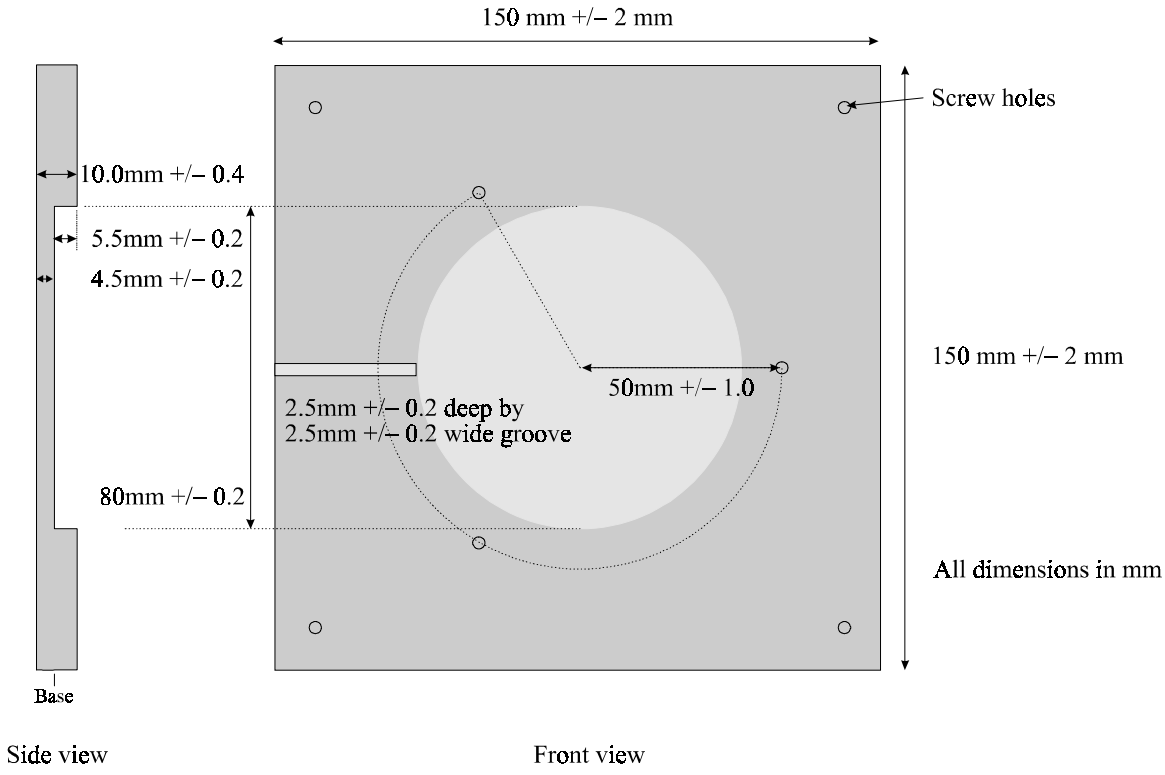

Figure 10 Backscatter chamber ‘phantom’

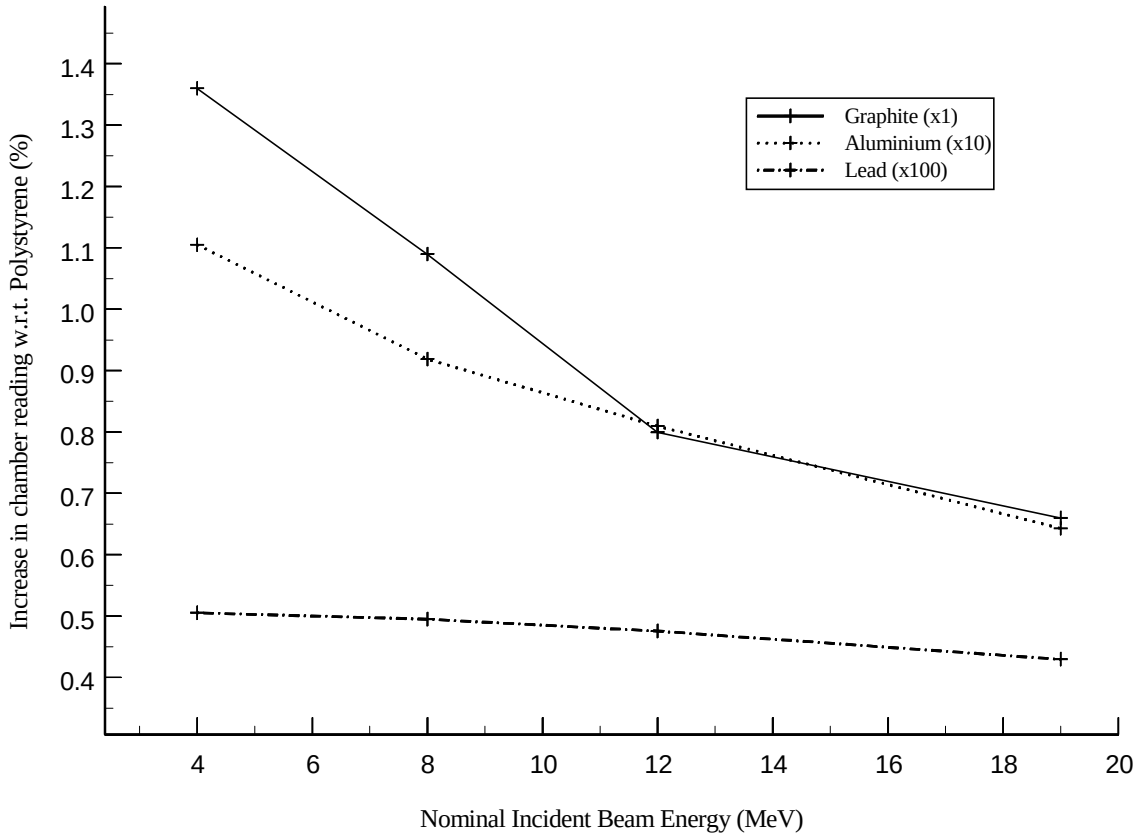

Figure 11 Backscatter experimental results

4.4 MONTE CARLO CALCULATIONS OF ELECTRON BACKSCATTER

The experimental measurements carried out in the previous section were modelled using an EGS4 user code. The user code was the same as that used to calculate the main perturbation factor calculations, namely a modified version of DOSRZ. The electron chamber was split up into 6 cylinders and 14 planes, as shown in **Figure 12** for 19 MeV electrons with graphite behind the chamber. The aluminium coating of the electrodes was not included in the simulation. In order to reduce the calculation time, zonal rejection was used, with PEGS data sets were created with AEs of 1, 10, and 200 keV. The radius of the outer cylinder was determined by adding the radius of the cavity (0.8 cm) to the csda range of the highest possible energy electron encountered in that particular simulation.

Calculations were performed at the nominal electron beam energies of 4, 8, 12, and 19 MeV, with the media behind the chamber being either air, aluminium, graphite, lead, or polystyrene. As for the main perturbation factor calculations, the calculation was split into three main stages.

4.4.1 Stage 1

The same phase space data files were used as for the perturbation factor calculations.

4.4.2 Stage 2

The stage 1 phase space data files were continued using the modified version of DOSRZ. The particle data was saved to disk as it crossed the boundary indicated in **Figure 12**.The stage 1

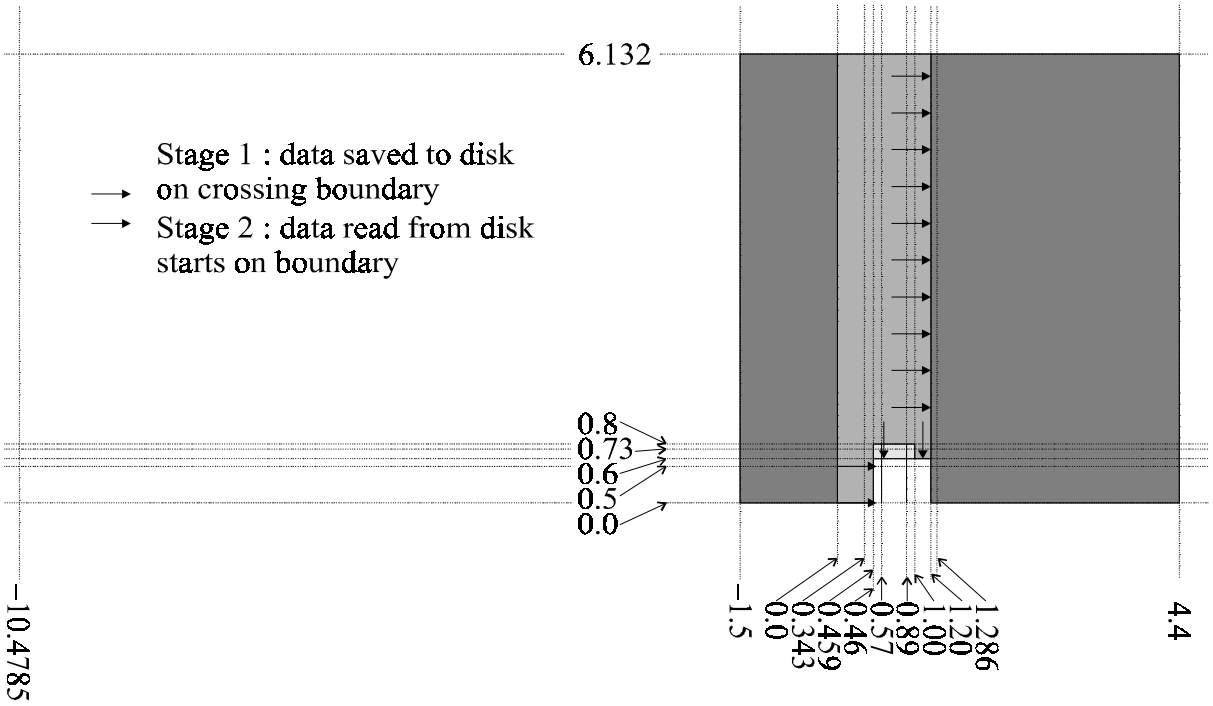

Figure 12 Geometry coding for backscatter chamber

phase space data was over-sampled up to ten times for each calculation. *ESTEPE* was set to the default 0.00, and *ECUT* to 0.512 keV.

4.4.3 Stage 3

The stage 2 phase space data files were continued again using the modified version of DOSRZ. Geometry coding for this stage was the same as for stage 2. The stage 2 phase space data was typically over-sampled eight times. *ESTEPE* was set to the default 0.00, and *ECUT* to 0.512 keV.

4.5 RESULTS

The results of the calculations are shown in **Table 6** and **Table 7** below. The back-scatter calculations do not agree with the back-scatter measurements. The calculations seriously under estimate the increase in dose in the chamber cavity, by as much as 30 % for low Z materials (polystyrene) to 100% for high Z materials (lead). Also, and more importantly, the ratio of graphite to polystyrene back-scatter is reversed. The measurements indicate that the backscatter from graphite is higher than that from polystyrene, while the calculations indicate the opposite.

	4 MeV	8 MeV	12 MeV	19 MeV
Polystyrene	1.046 ± 0.004	1.058 ± 0.005	1.06 ± 0.005	1.037 ± 0.011
Graphite	1.037 ± 0.006	1.046 ± 0.003	1.049 ± 0.007	1.029 ± 0.012
Aluminium	1.079 ± 0.006	1.093 ± 0.002	1.095 ± 0.006	1.065 ± 0.010
Lead	1.246 ± 0.018	1.318 ± 0.37	1.335 ± 0.007	1.284 ± 0.031

Table 6 Back-scatter measurements with respect to air

	4 MeV	8 MeV	12 MeV	19 MeV
Graphite	0.991 ± 0.004	0.988 ± 0.005	0.99 ± 0.005	0.992 ± 0.011
Aluminium	1.032 ± 0.005	1.033 ± 0.004	1.033 ± 0.006	1.027 ± 0.007
Lead	1.192 ± 0.016	1.246 ± 0.034	1.26 ± 0.005	1.238 ± 0.029

Table 7 Back-scatter measurements with respect to polystyrene

5. CONCLUSIONS

The values of the water to graphite cavity perturbation factor ratio were calculated to be approximately unity, with the assumption that any systematic errors cancelled out. In contrast, accurate measurements of wall perturbation factor could not be made using EGS4 and PRESTA (with the EGS4 parameter *ESTEPE* set to the default 0.00) because of large systematic backscatter errors that do not cancel. It remains to be seen whether using different values of *ESTEPE* will result in a more accurate calculation. It is hoped that the physical modelling within EGS4 will soon be improved: when this happens the codes, geometries and techniques described in this report will enable the efficient calculation of the perturbation factor to be performed. In the mean time however, the values of p_{wall} calculated here will not be used as part of NPL's new electron beam calibration service. Instead, a value of unity will be assumed, taken from the best data available to date, until further calculations are performed.

6. ACKNOWLEDGEMENTS

The authors would like to thank David Burns, formerly of NPL but now of the Bureau International des Poids et Mesures (BIPM), Paris, and Simon Duane for their help with this project. The authors would also like to acknowledge the financial support of the National Measurement Policy Unit of the UK Department of Trade and Industry.

7. REFERENCES

1. D.T. Burns, M.R. McEwen and A.J. Williams, *An NPL absorbed dose calibration service for electron beam radiotherapy* Proceedings of an international symposium on measurement assurance in dosimetry, Vienna, May 1993

2. A.E. Nahum, *Perturbation effects in dosimetry: Part I. Kilovoltage x-rays and electrons* Phys. Med. Biol **41** (1996) 1531-1580

3. C-M Ma and D.W.O. Rogers *Monte Carlo calculated wall correction factors for plane parallel chambers in high energy electron beams* Med. Phys **22** 672 (abstract)

4. ICRU *Radiation Dosimetry: Electron Beams with Energies Between 1 and 50 MeV* ICRU Report 35 (International Commission on Radiation Units and Measurements, Bethesda, Md.)

5. W.R. Nelson, H. Hirayama and D.W.O. Rogers, *The EGS4 code system* Stanford Linear Accelerator Center Report SLAC-265 1985

6. A.F. Bielajew and D.W.O Rogers, *The parameter reduced electron-stem algorithm for electron Monte Carlo transport* Nucl. Instrum. Methods B **18** 165-81

7. M.A. Hunt, G.J. Kutcher and A. Buffa, *Electron backscattering correction for parallel-plate chambers* Med Phys. **15** 96-103

APPENDIX A

This appendix lists the major modifications made to DOSRZ and other MORTRAN files to allow the code to be compiled using Lahey Fortran 90, and to added the alternative stopping power routines.

MODIFICATIONS TO ALLOW COMPILATION USING LF90

NRCC4MAC.MOR Version dated 90/03/30

`CALL EXIT` *changed to* `CALL EXIT(0)`

MACHINE.MAC Version dated 7-May-1996

Following lines added:

```
REPLACE{ALOG}WITH{LOG}

REPLACE{AMIN1}WITH{MIN}

REPLACE{AMAX1}WITH{MAX}

REPLACE{IFIX}WITH{INT}
```

MODIFICATIONS TO ADD ALTERNATIVE STOPPING POWERS

EGS4.MOR Version dated 95/9/5

Added `$ALTERNATIVE-SP-FLUORESCENCE` *macro at line 1519*

Changed `EDEP=PEIG` *to* `EDEP=E(NP)` *at line 1520*

DOSRZPAR.MOR Version dated 22-May-1996

```
"DENSITY RATIO SCALING MACRO (TO OVER-RIDE DENSITY IN A PARTICULAR REGION)"
REPLACE {$SET-RHOF;} WITH {RHOF=1;}
"         ========"
;
"MACROS TO ALLOW DIFFERENT STOPPING POWER DATA TO BE USED"
;
REPLACE {$EVALUATE DEDX0 USING EDEDX(ELKE)} WITH {
"         ================================"
DEDX0=EDEDX1(LELKE,MEDIUM)*ELKE+EDEDX0(LELKE,MEDIUM);
IF (MED_CAV(IRL).GT.0)[
    DEDX0_CAV=EDEDX1(LELKE,MED_CAV(IRL))*ELKE+EDEDX0(LELKE,MED_CAV(IRL));
    DEDX_CAV=RHOF*DEDX0_CAV;]}
;
REPLACE {$EVALUATE DEDX0 USING PDEDX(ELKE)} WITH {
"         ================================"
DEDX0=PDEDX1(LELKE,MEDIUM)*ELKE+PDEDX0(LELKE,MEDIUM);
IF (MED_CAV(IRL).GT.0)[
    DEDX0_CAV=PDEDX1(LELKE,MED_CAV(IRL))*ELKE+PDEDX0(LELKE,MED_CAV(IRL));
    DEDX_CAV=RHOF*DEDX0_CAV;]}
;
"THIS REPLACES THE PRESTA VERSION OF THE RE-EVALUATION TO ALLOW THE USE"
"OF DIFFERENT STOPPING POWER DATA THAN FOR THE MEDIA ACTUALLY USED.    "
;
REPLACE {$DEDX-RE-EVALUATION;} WITH
"         ==================="
{;IF(IEDEP=0)[
     DDXTMP=DEDX;EKETMP=EKE;ELKTMP=ELKE;
     EKE=EKETMP-DEDX*TVSTEP;
     ELKE=ALOG(EKE);
```

```
   $SET INTERVAL ELKE,EKE;
   IF(LELEC<0)[$EVALUATE DEDX01 USING EDEDX(ELKE);]
   ELSE       [$EVALUATE DEDX01 USING PDEDX(ELKE);]
   DEDX=RHOF*DEDX01;
   DEDX=0.5*(DDXTMP+DEDX);
   EKE=EKETMP;
   ELKE=ELKTMP;
   IF (MED_CAV(IRL).GT.0)[
       DDXTMP_CAV=DEDX_CAV;
       EKE_CAV=EKETMP-DEDX_CAV*TVSTEP;
       ELKE_CAV=ALOG(EKE_CAV);
       LELKE=EKE1(MED_CAV(IRL))*ELKE_CAV+EKE0(MED_CAV(IRL));
       IF(LELEC<0)[
         DEDX01_CAV=EDEDX1(LELKE,MED_CAV(IRL))*ELKE_CAV
         +EDEDX0(LELKE,MED_CAV(IRL));]
       ELSE       [
         DEDX01_CAV=PDEDX1(LELKE,MED_CAV(IRL))*ELKE_CAV
         +PDEDX0(LELKE,MED_CAV(IRL));]
       DEDX_CAV=RHOF*DEDX01_CAV;
       DEDX_CAV=0.5*(DDXTMP_CAV+DEDX_CAV);
       EDEP_CAV=DEDX_CAV*TVSTEP*RHO(MED(IRL))/RHO(MED_CAV(IRL));
    ]
]}
;
"THESE ADD EDEP_CAV WHEN ELEC/PHOTON IS DISCARDED"
;
REPLACE {EDEP=PEIE-PRM;} WITH
"        ============="
{EDEP_CAV=PEIE-PRM;EDEP=EDEP_CAV;}
;
REPLACE {EDEP=PEIE+PRM;} WITH
"        ============="
{EDEP_CAV=PEIE+PRM;EDEP=EDEP_CAV;}
;
REPLACE {$ALTERNATIVE-SP-FLUORESCENCE} WITH
"         ==========================="
{IRL=IR(NP);

IF (MED_CAV(IRL).GT.0)[
  IF (E(NP).LE.EBINDA(MED_CAV(IRL)))[EDEP_CAV=PEIG;]
  ELSE [
    EDEP_CAV=EBINDA(MED_CAV(IRL));
  ]
]
;}
;
"ADDS EDEP_CAV IN COMPTON ETC"
;
REPLACE {EDEP=PEIG} WITH
"        =========="
{EDEP_CAV=PEIG;EDEP=EDEP_CAV;}
```

Above lines added at line 581

```
REPLACE {;COMIN/EPCONT/;} WITH
   {;COMMON/EPCONT/EDEP,EDEP_CAV,TSTEP,TUSTEP,USTEP,TVSTEP,VSTEP,
     RHOF,EOLD,ENEW,EKE,ELKE,BETA2,GLE,TSCAT,
     IDISC,IROLD,IRNEW,IAUSFL($MXAUS);
    $ENERGY PRECISION EDEP,EDEP_CAV;}
```

Above lines added at line 889

```
REPLACE {;COMIN/MEDIA/;} WITH
  {;{SETR F=$FORTVER}
   [IF] {COPY F}=1977 [;
      COMMON/MEDIA/
         $LGN(RLC,RLDU,RHO,
         MSGE,MGE,MSEKE,MEKE,MLEKE,MCMFP,MRANGE,IRAYLM($MXMED)),NMED,
         MED_CAV($MXREG);
     COMMON/MEDIAC/MEDIA(24,$MXMED); $TYPE MEDIA;]
   [ELSE] [;
      COMMON/MEDIA/
         $LGN(RLC,RLDU,RHO,
```

```
            MSGE,MGE,MSEKE,MEKE,MLEKE,MCMFP,MRANGE,IRAYLM($MXMED)),NMED,
            MEDIA(24,$MXMED),MED_CAV($MXREG);]
    }
```

Above lines added at line 1009

Added `MEDIA` *to* `COMIN` *declaration at line 2031*

Changed `FTMP=WT(NP)*EDEP;` *to*

```
IF (MED_CAV(IRL).GT.0)[FTMP=WT(NP)*EDEP_CAV;]"uses this line for alt spowers"
ELSE                  [FTMP=WT(NP)*EDEP;]
```

at line 2081

Input card M3 substantially modified: now reads

```
"CARD M3
"*******

OUTPUT;(' *** INPUT CARD M3 ***');
MED(1)=0;CABSRB(1)=BLANK;DO I=2,NREG[MED(I)=1;CABSRB(I)=BLANK;] "DEFAULTS"
OUTPUT NREG;('0# OF GEOMETRICAL ZONES = ',I6,' ZONE(1) IS VACUUM(MED#=0)');
LOOP[
    MINPUT MEDNUM,ILOW,IHIGH,MED_CAVL;(4(1X,I6));
    WRITE(7,:M3:) MEDNUM,ILOW,IHIGH,MED_CAVL;
    :M3:FORMAT(' ',4(I6,' '));
    "DO SOME CHECKS FIRST"
    IF((ILOW.LE.0).OR.(ILOW.GT.NREG).OR.(IHIGH.LT.0).OR.(IHIGH.GT.NREG))[
        EXIT; "SIGNAL TO END MATERIAL INPUT LOOP"
        ]
    IF(MEDNUM.LT.0)[       MEDNUM=-1; "TOTALLY ABSORBING"    ]
    ELSEIF(MEDNUM.GT.NMED)[MEDNUM= 1; "DEFAULT TO 1st MEDIUM"]
    IF(IHIGH.LE.ILOW)[
        IF(MEDNUM.EQ.-1) CABSRB(ILOW)=ACHAR; "SET TOTALLY ABSORBING SWITCH"
        IF (MED_CAVL.GT.0)[
            OUTPUT ILOW,MEDNUM,MED_CAVL;
            (' REGION(',I4,')                = MATERIAL(',I2,'), USING STOPPING
 POWER DATA FOR MATERIAL(',I2,')');]
        ELSE[
              OUTPUT ILOW,MEDNUM;(' REGION(',I6,') = MATERIAL(',I2,')');]
        IF(MEDNUM.EQ.-1) MEDNUM=0; "SET TOTALLY ABSORBING REGION TO VACUUM"
        MED(ILOW)=MEDNUM;
        MED_CAV(ILOW)=MED_CAVL;
        ]
    ELSE[
        DO I=ILOW,IHIGH[
            IF(MEDNUM.EQ.-1) CABSRB(I)=ACHAR;] "SET TOTALLY ABSORBING SWITCH"
                IF (MED_CAVL.GT.0)[
                    OUTPUT ILOW,IHIGH,MEDNUM,MED_CAVL;
                    (' REGION(',I4,') TO REGION(',I4,') = MATERIAL(',I2,'), USIN
G STOPPING POWER DATA FOR MATERIAL(',I2,')');]
                 ELSE[
                    OUTPUT ILOW,IHIGH,MEDNUM;
                    (' REGION(',I6,') TO REGION(',I6,') = MATERIAL(',I2,')');]
        IF(MEDNUM.EQ.-1) MEDNUM=0; "SET TOTALLY ABSORBING REGION TO VACUUM"
        DO I=ILOW,IHIGH[
            MED(I)=MEDNUM;
            MED_CAV(I)=MED_CAVL;]
        ]
    ] "END OF REGION-MATERIAL INPUT LOOP"
$SKIP-LINE;
```